

# Starch Fractions as Examples for Nonrandomly Branched Macromolecules. 1. Dimensional Properties

Gabriela Galinsky and Walther Burchard\*

*Institute of Macromolecular Chemistry, University of Freiburg, 79104 Freiburg, Germany*

*Received October 4, 1994; Revised Manuscript Received January 18, 1995\**

**ABSTRACT:** Starch is well-known as a blend consisting of highly branched amylopectin and much smaller linear amylose. At a low amylose content the light scattering behavior is dominated by the amylopectin part. Applying a recent description by Fox and Robyt, a series of different molecular weights were prepared by acid degradation of potato starch. The obtained samples were characterized by static–dynamic light scattering and viscometry in a solution of 0.5 N NaOH. The results are compared with data from literature for amylose. The applicability of scaling relationships between exponents is checked. Determination of contraction factors allows evaluation of the branching density. These results are in good agreement with the theoretical model of ABC polycondensation. A comparison between the branching density obtained by LS measurements (0.016) and the branching density determined by NMR and enzymatical techniques (0.04) is made. The observed discrepancy is explained by a modified model of heterogeneously branched amylopectin. The approximate nature of the ABC model is also displayed by deviations of the experimental ( $\equiv R_g/R_h$ ) parameters from those predicted by the model.

## 1. Introduction

In the past the research on macromolecular solutions was mainly concerned with linear chain molecules in the dilute and semidilute regimes. Only in recent time have the properties of branched macromolecules been studied in detail, in particular regular star macromolecules.<sup>1–3</sup> The interest of many studies was focused on randomly branched macromolecules, the mechanism of gelation, and the critical behavior around the gel point.<sup>4–6</sup> The result from various systems was that percolation theory is obeyed in most cases, at least in the pregel states.<sup>7–12</sup>

In contrast, the present study deals with a system, which principally undergoes no gelation. Such structure is realized by amylopectin<sup>13</sup> and glycogen,<sup>14</sup> which are biopolymers formed by special enzymes, and in which the repeating unit is the  $\alpha$ -glucose.<sup>13–15</sup> This monomeric unit has the peculiarity that the OH groups in the C4- and C6-positions differ in reactivity from that in the C1-position, which as a half-acetal group has reducing functionality. In the course of biosynthesis  $\alpha(1,4)$ -glycosidic and  $\alpha(1,6)$ -glycosidic bonds are formed, this implies that the reducing end group in C1 can form a bond only with an OH group in the C4- or C6-position, but all other reactions are excluded. As pointed out already by Flory,<sup>16</sup> such systems cannot form a gel. This results from the constraints of limited possibilities of reaction, and these constraints cause significant deviations from randomness.

If a homogeneous reaction is assumed, the molar masses  $M_w$  and  $M_n$ , the radii of gyration  $R_g$ , and the particle scattering factor  $P(q)$  could be calculated<sup>17,18</sup> on the basis of cascade theory which is equivalent to special cases of the Flory–Stockmayer (FS) theory.<sup>16,19</sup> The biosynthesis excludes all possibilities of ring formation, and for this reason a better agreement of the FS theory with experimental data could be expected than for the random case, but the excluded volume effect is still not taken into account. Excluded volume effects essentially determine the fractal dimension of the branched clusters.<sup>5,20,21</sup> In the following we will assume the same values for the swollen and nonswollen branched clusters

of 2.0 and 2.5, respectively, as were deduced for random clusters by percolation theory.<sup>5</sup> The apparent fractal dimensions, however, will be different from those in randomly branched clusters. These values for the dimensions of individual clusters are modified by the huge width of the molecular size distribution in the random branching process.<sup>16</sup> However, for the present system the increase in polydispersity was predicted to be much smaller than for the random branching process,<sup>17,18</sup> such that the apparent fractal dimensions can be expected not to deviate too much from those of the individual clusters. In a series of three papers we report structural properties in the dilute and semidilute solutions from a number of starch fractions that were obtained by acid degradation of potato starch by applying a technique described by Fox and Robyt.<sup>22</sup> Starch is known to consist of two components, the branched amylopectin (an  $\alpha(1,4)\alpha(1,6)$ -glucan) and the linear  $\alpha(1,4)$ -linked glucan amylose. This composition makes interpretation of the results rather complex. Preliminary studies on various starches<sup>23</sup> revealed much larger dimensions of amylopectin than for the amylose, and since the amylose amount in potato starch does not exceed 22% (w/w), the effect of amylose proved to be very small.<sup>23</sup> Furthermore, by acid degradation also the amylose becomes hydrolyzed although with an apparently lower rate (Table 1, Figure 1).

The main intention of our study is a comparison of the conformational properties with those from the ABC polycondensation model that has been suggested as a good approximation for amylopectin and glycogen.<sup>24</sup>

In the present contribution (1) we confine ourselves to the dimensions of these macromolecules, their dependencies on molar mass, and the determination of contraction factors, which are characteristic parameters of the branching density. In a second paper (2) the angular dependences of the static and dynamic light scattering results are discussed, which give some insight into the internal structure and segmental mobility. Finally, the third paper (3) deals with the interaction among the macromolecules that depends on the molecular architecture (i.e. the osmotic modulus) and on association phenomena which are caused by H-bonding when the overlap concentration is exceeded.

\* Abstract published in *Advance ACS Abstracts*, March 1, 1995.

Table 1. Characteristic Parameters of Starch Fractions Obtained by Acid Hydrolysis in Alcoholic Suspensions<sup>a</sup>

	solvent	conc HCl V/mL	% IBC	% amylose content	DS/(±2)	$M_w/g\ mol^{-1}$ (±5%)	remarks
LD6	1-butanol	200	3.3 ± 0.6		97.3	72 000	precipitated, dried at 50 °C under vacuum
LD7	1-butanol	200	1.4 ± 0.4	2–3	87	32 000	
LD8	1-butanol	200	1.8 ± 0.2	4	91.5	35 400	defatted after degradation
LD9	1-propanol	200	2.9 ± 0.2	15	94.6	105 000	
LD10	methanol	200	3.3 ± 0.2	15	94.2	160 000	
LD11	methanol	100	4.3 ± 0.15	21	89.8	920 000	defatted before degradation
LD12	methanol	50	4.5 ± 0.2	22	90	5.2 × 10 <sup>6</sup>	
LD13	methanol	10	4.3 ± 0.15	21	93	9.7 ± 10 <sup>7</sup>	
LD14	methanol <sup>b</sup>	75	3.9 ± 0.3	19	88	320 000	
LD15	methanol <sup>b</sup>	150	2.7 ± 0.2	13	88.6	68 000	

<sup>a</sup> IBC = iodine binding capacity, DS = dry substance percentage,  $M_w$  = weight average molar mass. <sup>b</sup> Redistilled methanol (higher H<sub>2</sub>O content).

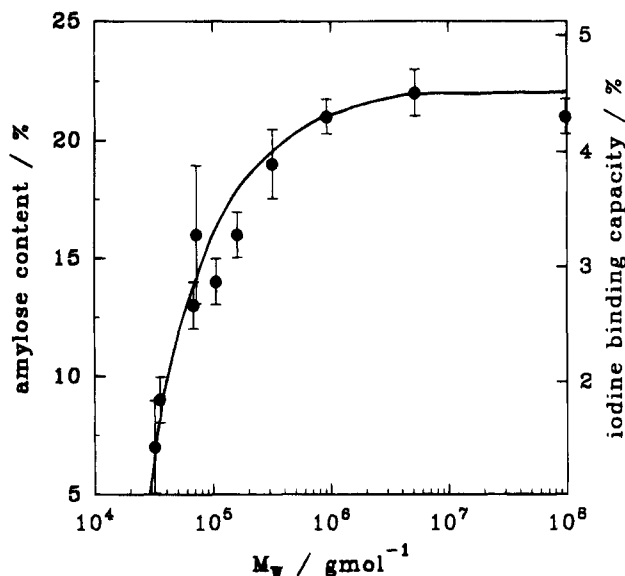


Figure 1. Iodine binding capacity (IBC) (right axis) and the resulting "amylose content" (left axis) for ten fractions of acid-degraded potato starches. An IBC of 20.5% at room temperature is taken as 100% amylose. Note: the decrease of IBC at low  $M_w$  does not necessarily indicate a decrease of the amylose content; the IBC of amylose also decreases, if the degree of polymerization becomes smaller than  $DP_w < 100$ . (See text.)

## 2. Experimental Section

**Starch Fractions.**<sup>22</sup> Potato starch from Cerestar, Vilvoorde, Belgium, was defatted by heating at 70 °C in a 1-propanol/water mixture of 3:1 for 10 h. During this time the solvent was changed three times. Then the starch (250 g) was suspended in 1 L of 1-butanol, 2-propanol, or methanol. To get different molecular mass fractions, between 200 and 10 mL of concentrated HCl was added to the samples at room temperature. Each mixture was shaken occasionally, and the reaction was stopped after 4 days when, according to literature, the limiting values should be reached.<sup>22</sup> The degraded starch was filtered and neutralized by washing with methanol/water (1:1). To the first wash solution some NaOH was added.

**The dry substance content (DS)** was around 90% for each sample. It was determined by drying the starches under vacuum at 90 °C in the presence of P<sub>2</sub>O<sub>5</sub>.

**The amylose content** was determined by the iodine-binding capacity (IBC), which was measured by potentiometric titration<sup>14</sup> with a titroprocessor 636 from Metrohm.

**The number average molecular mass ( $M_n$ )** was obtained according to Nelson–Somogyi<sup>25</sup> by determining the number of reducing end groups. Three solutions are needed for this test.

Solution A: 25 g of Na<sub>2</sub>CO<sub>3</sub>, 25 g of K–Na–tartrate·4 H<sub>2</sub>O, 20 g of NaHCO<sub>3</sub>, 200 g of Na<sub>2</sub>SO<sub>4</sub> in 1 L of water.

Solution B: 15 g of Cu<sub>2</sub>SO<sub>4</sub>·5H<sub>2</sub>O and 2 drops of concentrated H<sub>2</sub>SO<sub>4</sub> in 100 mL of water.

Solution C: (a) 25 g of (NH<sub>4</sub>)<sub>6</sub>Mo<sub>7</sub>O<sub>24</sub>·4H<sub>2</sub>O, 21 mL of concentrated H<sub>2</sub>SO<sub>4</sub> in 450 mL of water; (b) 3 g of Na<sub>2</sub>HAsO<sub>4</sub>·7H<sub>2</sub>O in 25 mL of water; (a) and (b) have to be combined and stored in a dark flaked bottle.

**Copper reagent:** 25 mL of solution A and 1 mL of solution B, freshly prepared.

A 1 mL aliquot of the sample solution (i.e. 5 g/L oligosaccharides) and 1 mL of copper reagent are combined and boiled in a water bath for 20 min. Then the solution is cooled for 5 min with cold water, and 1 mL of solution C is added. Now the solution has to be shaken strongly, and after 5 min the solution is filled to 10 mL. The absorbance is measured at a wavelength at 540 nm. Maltotriose and a standard dextrane ( $M_n = 26\ 000\ g/mol$ ) were used for establishing the calibration curve.

**Viscosity** measurements were carried out in 0.5 N NaOH at 20 °C with an automatic Ubbelohde viscometer (Schott) using a capillary of 0.63 mm.

**Static light scattering** measurements were performed at 20 °C with a fully computerized and electronically modified SOFICA photogoniometer (Baur, Instrumentenbau, Hausen, Germany) in the angular range from 30 to 140° in steps of 5°. An argon ion laser ( $\lambda_0 = 488\ nm$ ) was used as the light source.

**Dynamic light scattering** measurements were made with an automatic ALV goniometer and an ALV 3000 correlator/structurator in the single- $\tau$  mode (from 30 to 150° in steps of 5°). The light source was a Spectra Physics argon ion laser ( $\lambda_0 = 496.5\ nm$ ).

The solutions were filtered through Millopore filters (0.22  $\mu m$ , for samples with  $M_w < 4.5 \times 10^6\ g/mol$ , and through 0.8 and 1.2  $\mu m$  for  $M_w = 90 \times 10^6\ g/mol$ ). A refractive index increment of 0.142 was used.<sup>26</sup>

## 3. Results

Ten fractions of degraded potato starch were prepared by acid hydrolysis of alcoholic starch suspensions, as described in the Experimental Section. Methanol, 1-propanol, and 1-butanol were used. The strongest degradation was obtained in 1-butanol, and the weakest, in methanol.<sup>22</sup> Only for the lowest molecular weights were 1-butanol and 1-propanol applied; in all other cases the HCl molarity was changed. The incubation time of 4 days was kept constant in all experiments.

Of these samples the molar masses  $M_w$ , the radii of gyration  $R_g$ , and the second virial coefficients  $A_2$  were measured by static LS (see Figure 2); the diffusion coefficients  $D_z$  and the corresponding hydrodynamic radii  $R_h$  were determined by means of dynamic LS. The results of  $R_g$  and  $R_h$  and the ratios of both,  $\rho = R_g/R_h$  are shown in Figure 3. The radii of gyration for the two lowest samples could not be measured since the sizes were smaller than 15 nm. The hydrodynamic radii

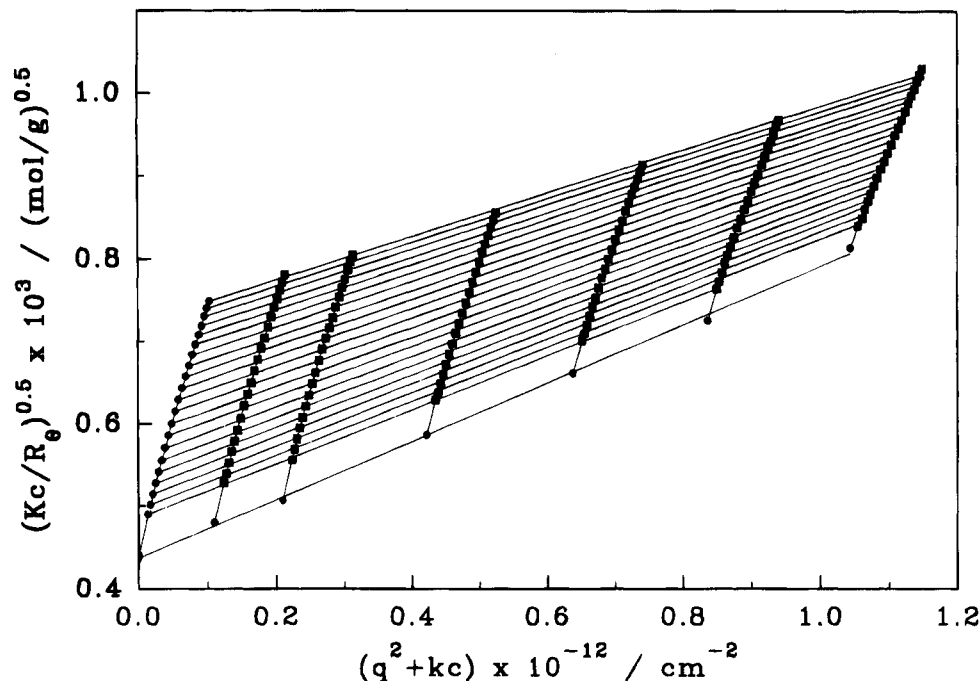


**Figure 2.** Berry plot  $((Kc/R_g)^{0.5})$  of a degraded starch in 0.5 N NaOH for concentration up to 0.6 to 6 g/L.  $M_w = 5.2 \times 10^6$  g/mol,  $A_2 = 2.7 \times 10^{-5}$  (mol mL)/g,  $R_g = 70$  nm.

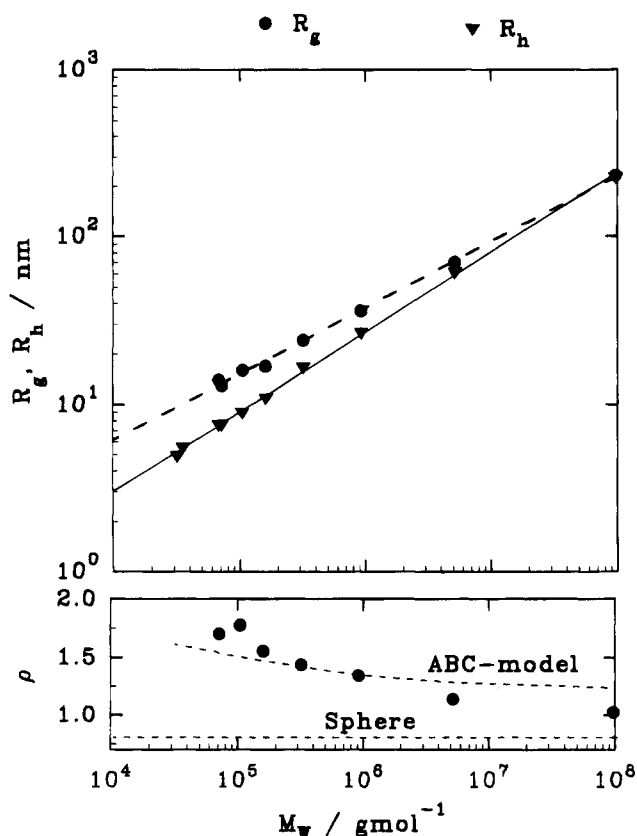


**Figure 3.** Radius of gyration  $R_g$  and hydrodynamic radius  $R_h$  in 0.5 N NaOH as a function of molar mass  $M_w$  for the partially degraded potato starches. Underneath:  $\rho = R_g/R_h$  parameter. The broken lines correspond to models of ABC polycondensation and hard sphere behavior.

were calculated from the diffusion coefficients via the Stokes–Einstein equation.

$$D_z = \frac{kT}{6\pi\eta} \left\langle \frac{1}{r_{hz}} \right\rangle \quad R_h \equiv \left[ \left\langle \frac{1}{r_{hz}} \right\rangle \right]^{-1} \quad (1)$$

Strikingly, the curves for  $R_g$  and  $R_h$  have not the same slopes (which are  $\nu_g = 0.394$  and  $\nu_h = 0.476$ , respectively, in the relationship  $R_{g,h} \sim M_w^{\nu_{g,h}}$ ), while for linear chains parallel lines are generally found.<sup>27</sup> Correspondingly, the  $\rho$  parameter

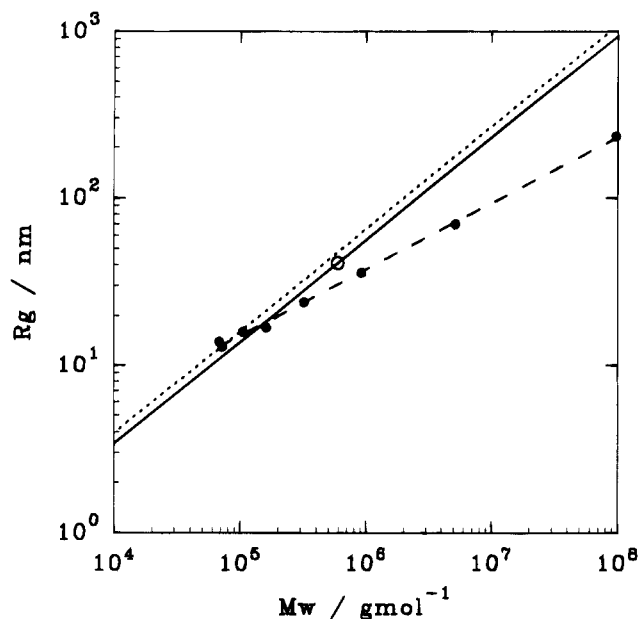
$$\rho = R_g/R_h \quad (2)$$

was found to decrease with increasing molecular mass from a value which is characteristic for linear chains to a value which is typical for a star-branched macromolecule with a large number of arms.<sup>1,2</sup>

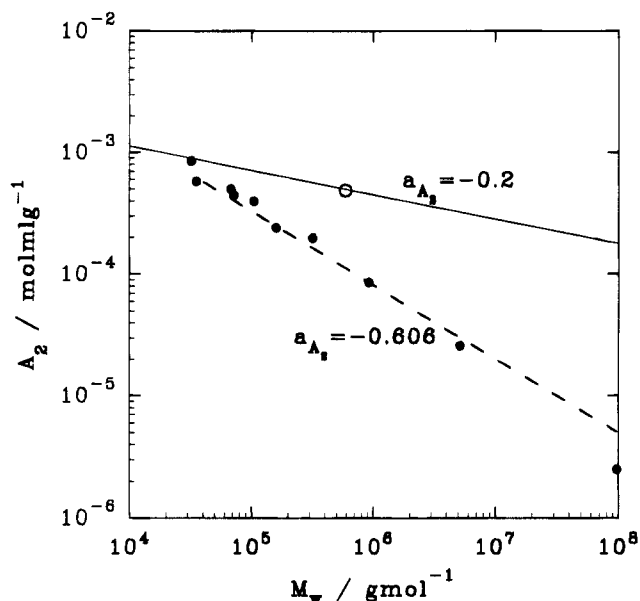
It is of interest to compare the molar mass dependence of the radius of gyration of the branched materials with that for linear amyloses. Unfortunately, only one point is known from literature.<sup>28</sup> However, assuming validity of scaling relationships,<sup>21</sup> the exponent of  $\nu$  of the molar mass dependence for  $R_g$  can be estimated from the exponent of the intrinsic viscosity  $a_{[\eta]} = 3\nu - 1$ . With the value of  $a_{[\eta]} = 0.84$  one obtains  $\nu = 0.61$  which is slightly higher than for flexible linear chains in a good solvent (0.5918).<sup>29</sup> The solid line drawn in Figure 4 was calculated from the point of measurement (synthetic, monodisperse amylose) and with a slope of 0.61. Strikingly, these two lines intersect at a molecular mass of around 200 000 g/mol. Because amylopectin fractions are polydisperse, it is better to compare these with polydisperse amyloses. To compute this line, the curve has to be multiplied by  $(3/2)^{1/2}$  (Schulz–Flory distribution  $\langle R_g^2 \rangle_z : \langle R_g^2 \rangle_w = 3:2$ ).

Figure 5 shows the results of the second virial coefficients which are compared with the behavior for linear chains. Exponents of  $-0.61$  and  $-0.2$  were obtained for the branched and linear glucan architectures. The curve for the linear chain was calculated from scaling relationships (see eq 3) and was drawn through the point known from literature.<sup>28a</sup>

The results of viscosity measurements are given in Figure 6; they are again compared with linear fractions.<sup>28b</sup> The corresponding exponents are 0.39 and 0.84 for the branched and linear samples. The intrinsic



**Figure 4.** Comparison of the radii of gyration of the branched fractions with those of linear amyloses of the same molar mass. The full line corresponds to uniform synthetic amyloses, the dotted one, to polydisperse (most probable distribution) linear chains. The filled circles and broken line represent the results from the degraded starches.



**Figure 5.** Molar mass dependence of the second virial coefficient  $A_2$  for the branched fractions (●) and linear amyloses (○).

viscosity of amylose is always larger than that of the branched fractions. To estimate the polydispersity of the various fractions, we measured in addition to  $M_w$  from LS the number average  $M_n$  by end group determination applying the Nelson–Somogyi method. The polydispersity was found to increase with  $M_w$ , as shown in Figure 7.

#### 4. Discussion

**Some General Remarks.** Before the conformational properties are discussed, it has to be stressed that starch is actually a blend of a highly branched component with a linear component of the same chemical composition. In addition the branched macromolecules are much

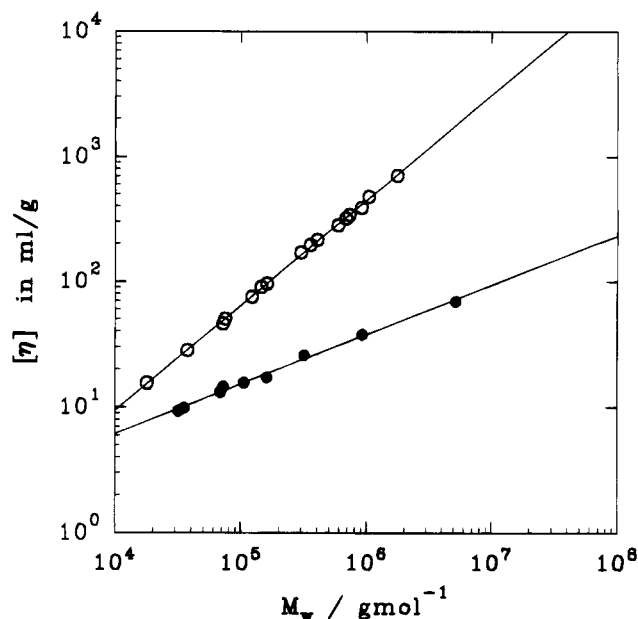


**Figure 6.** Molar mass dependences of the intrinsic viscosities for the branched starch fractions (●) and linear amylose (○) in 0.5 N NaOH at 20 °C.

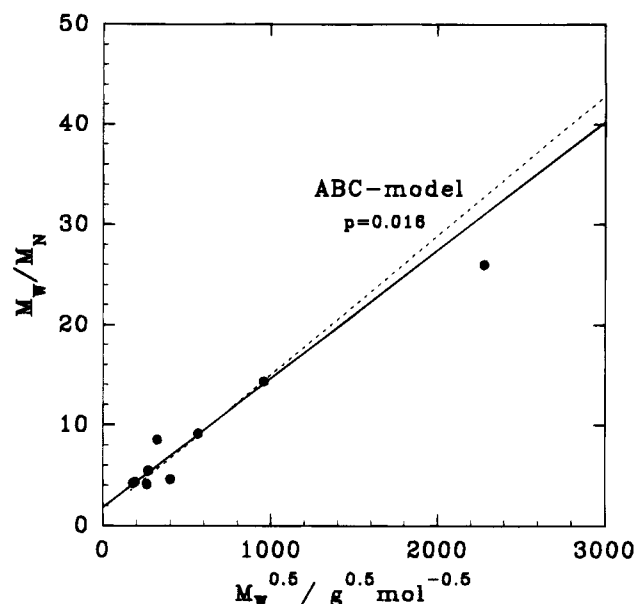


**Figure 7.** Polydispersity index  $M_w/M_n$  as a function of the root weight average molar mass for the degraded starches. The dotted line results from the predictions of the ABC polycondensation model with a branching density of  $p = 0.016$ . For further details, see text.

larger in size and molar mass than the linear fractions such that the conformation properties are dominated by the branched molecules.<sup>23</sup>

A special situation occurs when the starch is degraded. According to Figure 1 the amylose content as determined by iodine-binding capacity (IBC) seems to stay constant over 2 decades in molar mass, but then apparently decreases. From this behavior it might be concluded that amylose is much more stable against hydrolysis than the branched amylopectin. It is known, however, that the IBC becomes independent of chain length if a critical degree of polymerization of about 100 is exceeded, and therefore the degradation of amylose cannot be followed quantitatively. Also spectroscopy of the iodine complexes could not satisfactorily be applied

since the characteristic bands of amylose are highly perturbed by the broad bands of amylopectin which at 80% is the major component. On the other hand, the strong decrease does not necessarily indicate a disappearance of amylose. On the contrary, an increase of oligomeric linear chains with negligible IBC has to be expected which originates also from the degraded branched fractions. Surprisingly, the branched amylopectin in the grain is partially crystalline<sup>13</sup> and thus the hydrolysis will preferentially occur in the amorphous transition zones near the branching points. This effect will be responsible for an increase of oligomeric linear chains.

The reason the amylose appears to be more stable against hydrolysis than amylopectin may be understood by the facility of helical complex formation with the alcohols used as the suspension medium.

**Global Structure.** The first question that has to be answered is what the reason may be for the different slopes of  $R_g$  and  $R_h$ . There are principally two possibilities: (i) polydispersity or (ii) change of the branching structure. Model calculations have shown that the ratio  $\rho = R_g/R_h$  decreases with branching for monodisperse clusters.<sup>1,30</sup> On the other hand, polydispersity has a stronger influence on  $R_g$  than on  $R_h$ , and thus the  $\rho$  parameter increases with polydispersity.<sup>30</sup> Therefore, in the actual branched system the effect of branching (decrease of  $\rho$ ) is partially compensated by the effect of polydispersity. For randomly branched systems the two effects are fully balanced and the  $\rho$ -parameter remains constant in the whole  $M_w$  region.<sup>1,30</sup> Measurements with the starch samples gave considerably lower values, indicating a much narrower molar mass distribution. Hence, the influence of polydispersity is here less than the effect of branching and the decrease of  $\rho$  indicates an increase of branching points per macromolecules.

It is worth mentioning that a similar decrease was predicted<sup>31</sup> and experimentally found<sup>32</sup> for regular star-branched macromolecules, which confirms that an increase of branching accompanied with a weak increase of polydispersity is the essential reason for the strikingly different slopes in Figure 3. In fact, model calculation on the basis of the Flory–Stockmayer theory for the ABC or AB<sub>2</sub> polycondensation<sup>18</sup> predicted the observed decrease of  $\rho$  with increasing molar mass, when the number of branches is taken as an adjustable parameter. A quantitative agreement is not to be expected since the mentioned calculations were based on Gaussian statistics for the chain sections connecting two arbitrary pairs of monomeric units in the branched macromolecules. Excluded volume effects were not taken into account. A more detailed discussion of this approximation will be given in paper 2, where the fractal dimensions of the polymers are considered.

**Interrelationship between the Various Exponents of the Molar Mass Dependence.** In the limit of good solvent behavior the exponents of linear chains for the radii ( $\nu$ ), intrinsic viscosity ( $\alpha_{[\eta]}$ ), and the second virial coefficient ( $\alpha_{A_2}$ ) obey scaling relationships,<sup>21</sup> which are

$$\begin{aligned}\alpha_{[\eta]} &= 3\nu - 1 \\ \alpha_{A_2} &= 3\nu - 2\end{aligned} \quad R_h, R_g \sim M^\nu \quad (3)$$

where it is of no influence whether the exponents  $\nu_g$  or  $\nu_h$  from the  $R_g$  or  $R_h$  dependences is taken.

It is of interest to check whether similar scaling relationships hold also for the branched materials. Here

**Table 2. Exponents of Scaling Relationships (See Eq 3) with an Error of around  $\pm 0.01^a$**

	branched			linear
	exptl	calcd from		
		$\nu_{R_g}$	$\nu_{R_h}$	
$a_{[\eta]}$	0.39	0.18	0.43	0.84 (0.775)
$a_{A2}$	-0.61	-0.82	-0.57	(-0.2246)
$\nu_{R_g}$	0.39			0.61 (0.5918)
$\nu_{R_h}$	0.48			0.61 (0.5918)

<sup>a</sup> The data in brackets denote the theoretically expected values for linear flexible chains.

it makes a difference whether  $\nu_g$  or  $\nu_h$  is taken. The measured exponents  $\alpha_{[\eta]}$  and  $\alpha_{A_2}$  together with the calculated ones are listed in Table 2. In this simple-minded picture the exponent for the hydrodynamic radius gives a better agreement with experiment, while for values based on  $\nu_g$  a significantly lower exponent is obtained than measured. In fact, the validity of the scaling laws cannot be expected for the following reasons.

Assuming the Fox–Flory approach<sup>33</sup> to be valid also for branched polymers, we can write for polydisperse samples<sup>34</sup>

$$[\eta]_b = \Phi_b \frac{(R_g^3)_n}{M_n} \quad (4)$$

The scaling laws can only be expected when  $\Phi_b$  and also the polydispersity remains constant for the various samples of the present study. The polydispersity increases, however, roughly with the root of the molecular mass (Figure 7), as was predicted for the ABC polycondensation model.<sup>17</sup> The ratio of the two number averages in eq 4 is very close to a quantity that is almost independent of polydispersity and approximately corresponds to a number average for  $[\eta]$ . If this quantity is plotted against  $M_w$  rather than  $M_n$ , then the curve in Figure 5 must become flatter as  $M_w/M_n$  increases with  $M_w$ ; such behavior is indeed observed but the measured exponent is larger than derived from  $\nu_{R_g}$  with the scaling relationship (3). Consequently, the draining parameter  $\Phi_b$  must increase with the particle size; e.g. the solvent can penetrate less deeply into the coil as the particle sizes increases. Exactly such behavior could be expected for growing clusters of the same branching density.

The exponent for  $A_2$  can be discussed as follows. In the limit of a good solvent the second virial coefficient can be written as<sup>3,35</sup>

$$A_2 = 4\pi^{3/2} N_A \frac{R_g^3}{M^2} \Psi_b^* \quad (5)$$

When polydispersity is neglected, the interpenetration function  $\Psi_b^*$  of the branched material may increase with the number of branches and thus with the molecular mass; i.e. the interpenetration of branched clusters will decrease as the number of branches increases. For this reason the exponent resulting from eq 3 should be more negative than experimentally found, and this is indeed observed. It is of interest that the exponent  $\alpha_{A_2}$  calculated from  $\alpha_{[\eta]}$  (eq 3) gives a satisfactory agreement with experimental finding. From this effect we can conclude that the increase of  $\Phi_b$  with the molecular weight is the same as that of  $\Psi_b^*$ . The ratio of these two quantities ( $A_2 M_w / [\eta]$ ) is approximately 2 in contrast to linear chains where a ratio of about 1 was found.<sup>3,35</sup>

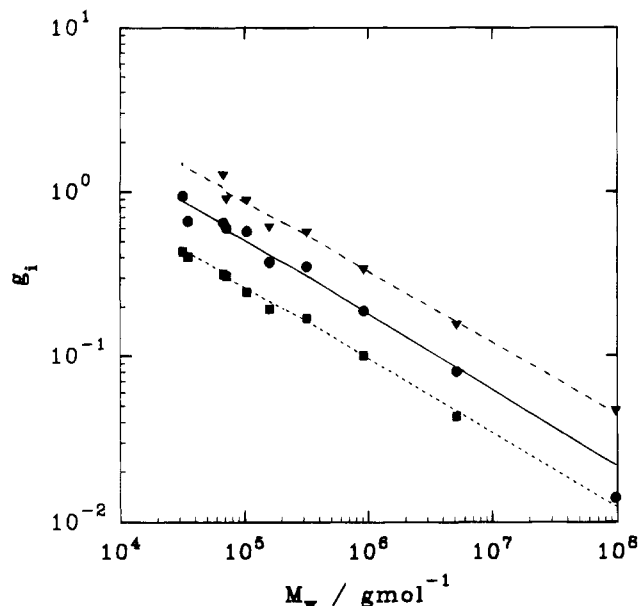


**Figure 8.** Molar mass dependences of contraction factors  $g_i$  ( $i = (\nabla) R_g^2$ ,  $(\bullet) A_2$ ,  $(\blacksquare) [\eta]$ , respectively; see eq 6).

The same ratio of about 2 was found by Bauer and Burchard<sup>36</sup> with fractionated polycyanurates.

It may be noted that the experimental points of  $A_2$  for the highest molecular weights appear to fall below the drawn line. Similar behavior has been observed with the branched epoxy resins<sup>37</sup> by Wachenfeld et al. and with the polycyanurates mentioned above. This deviation seems to be a general feature for which we have so far no explanation.

**Contraction Factors.** By comparison of a linear chain with a highly branched structure of the same molecular mass it is obvious that the branched molecule has a smaller dimension than the linear one. This effect led Stockmayer and his co-workers to introduce contraction factors for the mean square radii of gyration<sup>38</sup>  $g = R_{g,br}^2/R_{g,lin}^2$  and the viscosities<sup>39</sup>  $g' = [\eta]_{br}/[\eta]_{lin}$ . In addition to these contraction parameters another one can be introduced that is based on the second virial coefficient.<sup>40</sup> In this paper we rename the parameters as follows:

$$\begin{aligned} g_{R_g^2} &= \frac{R_{g,br}^2}{R_{b,lin}^2} \\ g_{[\eta]} &= \frac{[\eta]_{br}}{[\eta]_{lin}} \\ g_{A_2} &= \frac{A_{2,br}}{A_{2,lin}} \end{aligned} \quad (6)$$

These quantities are plotted against  $M_w$  in Figure 8. Three essentially parallel lines are obtained which appear shifted by a constant factor of approximately 1.5 for  $A_2$  and 3 for  $[\eta]$ . In other words,  $g_{A_2}$  and  $g_{[\eta]}$  increase linearly with  $g_{R_g^2}$  but do not approach the value 1 at  $g_{R_g^2} = 1$ . The observation of three parallel lines for the different  $g$  factors could be explained by changes of the penetration functions  $\Phi_b$  and  $\Psi_b^*$ . It was expected that the curves meet each other at a value of unity for low molecular weights, since the molecules have been completely degraded to linear chains, if the degradation solely consists of debranching. However, the acid

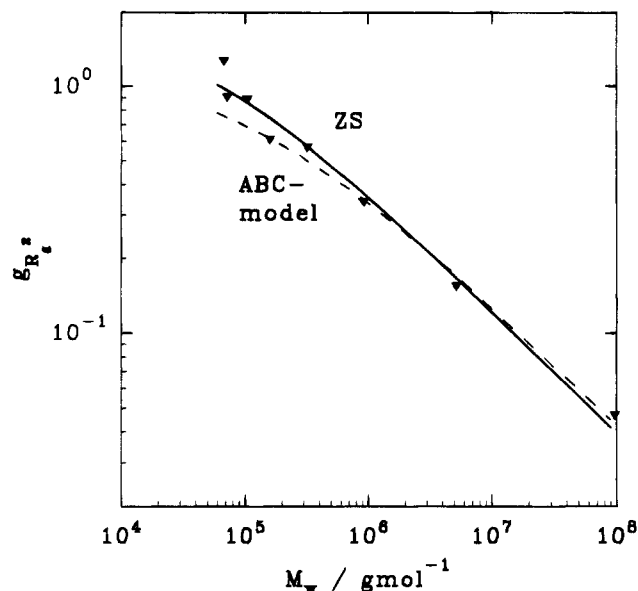


**Figure 9.** Comparison of experimental  $g_{R_g^2}$  contraction factors with theoretical predictions by Zimm and Stockmayer<sup>38</sup> and from the ABC polycondensation model.<sup>1,18</sup> The only fitting parameter is the number of branches per macromolecule  $B/DP_w$ .

degradation occurs statistically, and this means that linear and branched compounds remain present in the system, even at low  $M_w$ . A theory which quantitatively could explain this behavior is missing. Only the  $g_{R_g^2}$  factor relationships have been derived by Zimm and Stockmayer<sup>38</sup> and by one of us,<sup>1,23</sup> respectively, which are given in eqs 7 and 8, where  $B$  denotes the number of branching points per weight average degree of polymerization of the macromolecule.

$$g_{ZS} = \frac{3}{2[(1 + B/7)^{1/2} + 4B/9\pi]^{1/2}} \quad (7)$$

$$g_B = \frac{6[2 + (1 + 2B)^{1/2}]}{[3 + (1 + 2B)^{1/2}]^2} \quad (8)$$

In ref 1 the number average number of branching points was given and was here converted to the weight average. In spite of different approaches the two theories give very similar results (Figure 9). Only at short chains are deviations noticeable. Surprisingly, these theories fit the exponential data satisfactorily well. Thus, it is tempting to use these equations for the estimation of the number of monomeric units, belonging to linear chain sections, per branching point ( $P_w/B$ ). Values of  $63 \pm 2$  and  $67 \pm 2$ , respectively, were obtained from the fits. The meaning of these data is discussed below.

**$\varrho$  Parameter.** Knowing the data for  $P_w/B$ , one can also calculate the  $\varrho$  parameter with the ABC model without assumptions of additional fitting parameters.<sup>1</sup> The result is shown in Figure 2 as a broken line. The theoretical curve displays the correct tendency but does not fully fit the experimental data. The experimentally determined values lower than predicted in the asymptotic region of high  $M_w$  correspond to earlier findings with star-branched macromolecules<sup>32</sup> and could eventually be understood by the Monte Carlo calculations of Rey et al.<sup>41,42</sup> The increase at low  $M_w$  weaker than found experimentally cannot be explained by this argument and has its basis in an incorrect model.

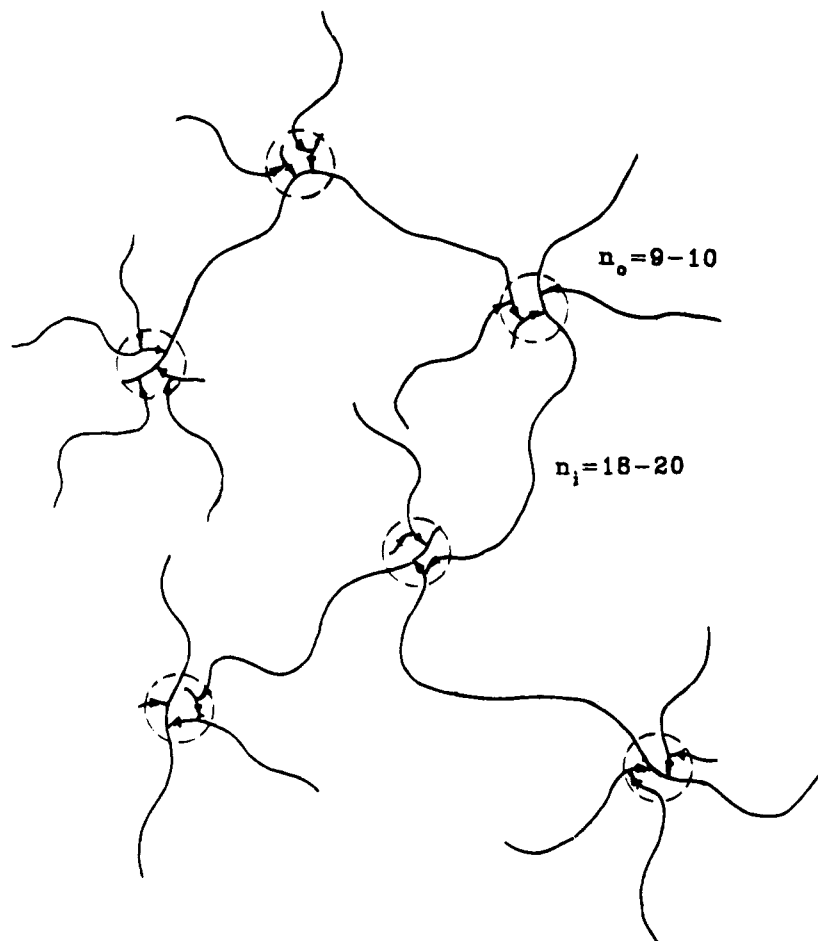


**Figure 10.** Model of heterogeneously branched amylopectin, assuming 4.5 branches per nodule of which 3.5 are outer chains of chain length  $x$  and one inner chain (connecting two nodules) of chain length  $2x$ , such that  $66 = 5.5x$ . If the dimension of the highly branched nodule is taken into account,  $x$  reduces by 2 units. The length of outer chains was found to be 9–10 anhydroglucoses, and that of inner chains, to be twice as large.

**Polydispersity.** The mentioned ABC polycondensation model allowed derivation of the polymer dispersity as a function of  $M_w$ . The dotted line in Figure 7 represents the result, while the solid line displays the best fit. A surprisingly good agreement can be stated.

## 5. Conclusions

With the value of  $P_w/B$  the branching probability (i.e. the extent of reaction of the C group) can be calculated, which is  $p = B/P_w$ . This gives a value of 0.016 which is about 2.5 times smaller than found from enzymatical degradation and by NMR techniques. In fact, the simple ABC model was found by Robin and Mercier<sup>43</sup> not to be valid. They found a heterogeneously branched structure where about 9 long chains are grafted onto small branching nodules. Most of them are outer chains; only a few branch off. The nodules consist of a small domain with a high branching density ( $p = 0.5$ ) where on average every second glucose unit forms a branching point. Later calculations by Thurn and Burchard<sup>44</sup> predicted a smaller number of 4–5 branches per nodule. A possible structure in space is schematically illustrated by Figure 10.

Complete debranching should now result in a large fraction of outer chains ( $8x$ , respectively  $3.5x$ , where  $x$  is the degree of polymerization of one outer chain) and a smaller one of inner chains with a chain length that is twice as large. For the Robin–Mercier model we find an outer chain length of about 6–7 units, while for the

Thurn–Burchard model a value of 11–12 units is obtained (see description to Figure 10). If the dimension of the highly branched nodule is taken into account, this length reduces to 9–10 units. The second approach agrees apparently better with results from literature.<sup>45</sup>

In view of the rather complex heterogeneous structure which was concluded from specific enzymatic degradation experiments, it remains surprising that the simple ABC model in principle shows the correct behavior. One explanation for this observation may be found in the small size of the nodules compared with the wavelength of the light and the length of the branches.

**Acknowledgment.** The authors benefitted from help by Dr. Waltraud Vorwerg, Fraunhofer-Institute of Applied Polymer Research, Teltow, who kindly provided us with the techniques of quantitative amylose content determination, which is gratefully acknowledged. Financial support was given by the Deutsche Forschungsgemeinschaft.

## References and Notes

- (1) Burchard, W. *Adv. Polym. Sci.* **1983**, *48*, 1.
- (2) Bywater, S. *Adv. Polym. Sci.* **1979**, *30*, 89.
- (3) (a) Freed, K. F. *Renormalization Group Theory of Macromolecules*; Wiley & Sons: New York, 1987. (b) Cherayil, B. J.; Bawendi, M. G.; Miyake, A.; Freed, K. F. *Macromolecules* **1986**, *19*, 2770. (c) Douglas, J. F.; Roovers, J.; Freed, K. F. *Macromolecules* **1990**, *23*, 4168. (d) Douglas, J. F.; Freed, K. F. *Macromolecules* **1984**, *17*, 2344.

- (4) Stauffer, D.; Coniglio, A.; Adam, M. *Adv. Polym. Sci.* **1982**, *44*, 103.
- (5) Stauffer, D. *Introduction to Percolation Theory*; Taylor & Francis: London, Philadelphia, 1985.
- (6) (a) Gordon, M. *Proc. R. Soc. London, Ser. A* **1962**, *268*, 240. (b) Gordon, M.; Malcolm, G. N.; Butler, D. S. *Proc. R. Soc. London, Ser. A* **1966**, *295*, 29. (c) Gordon, M. In *Gels. Gelling Processes. Faraday Discuss. Chem. Soc.* **1974**, *57*, 1.
- (7) Adam, M.; Delsanti, M.; Munch, J. P.; Durand, D. *J. Phys. (Paris)* **1987**, *48*, 1809.
- (8) Schosseler, F.; Benoit, H.; Grubisic-Gallot, Z.; Strazielle, C.; Leibler, L. *Macromolecules* **1989**, *22*, 400.
- (9) Patton, E. V.; Wesson, J. A.; Rubinstein, M.; Wilson, J. C.; Oppenheimer, L. E. *Macromolecules* **1989**, *22*, 1946.
- (10) Bauer, J.; Lang, P.; Burchard, W.; Bauer, M. *Macromolecules* **1991**, *24*, 2634.
- (11) Trappe, V.; Richtering, W.; Burchard, W. *J. Phys. II (Paris)* **1992**, *2*, 1453.
- (12) (a) Trappe, V. Ph.D. Thesis, Freiburg, 1994. (b) Trappe, V.; Burchard, W. *Polymer Prepr. (Am. Chem. Soc., Div. Polym. Chem.)* **1994**, *36*, 1.
- (13) (a) Aspinall, G. O. *Polysaccharides*; Pergamon Press: Oxford, New York, 1970. (b) Guilbot, A.; Mercier, Ch. In *Starch*; Aspinall, G. O., Ed.; The Polysaccharides Vol. 3; Academic Press: London, New York, 1985.
- (14) Banks, W.; Greenwood, C. T. *Starch and its Components*; University Press: Edinburgh, 1975.
- (15) Whistler, R. L.; BeMiller, J. N.; Paschall, E. F., Ed. *Starch, Chemistry and Technology*; Academic Press: London, New York, 1984; Chapters V and VI.
- (16) Flory, P. J. *Principles of Polymer Chemistry*; Cornell University Press: Ithaca, NY, 1953.
- (17) Burchard, W. *Macromolecules* **1972**, *5*, 604.
- (18) Burchard, W. *Macromolecules* **1977**, *10*, 919.
- (19) Stockmayer, W. H. *J. Chem. Phys.* **1943**, *11*, 45; **1944**, *12*, 125.
- (20) Isaacson, J.; Lubensky, T. C. *J. Phys. (Paris)* **1980**, *41*, L469.
- (21) de Gennes, P.-G. *Scaling Concepts in Polymer Physics*; Cornell University Press: Ithaca, NY, 1979. *C. R. Acad. Sci. (Paris)* **1980**, *291*, 17.
- (22) Fox, J. D.; Robyt, J. F. *Carbohydr. Res.* **1992**, *227*, 163.
- (23) Aberle, Th.; Burchard, W.; Vorwerg, W.; Radosta, S. *Starch / Staerke*, in press.
- (24) Reference 1, pp 31 and 72.
- (25) Nelson, N. *Z. Biol. Chem.* **1944**, *153*, 375.
- (26) Huglin, M. L., Ed. *Light Scattering from Polymer Solution*; Academic Press: London, New York, 1972.
- (27) Schmidt, M.; Burchard, W. *Macromolecules* **1981**, *14*, 210.
- (28) (a) Burchard, W. *Makromol. Chem.* **1963**, *59*, 16; (b) **1968**, *64*, 110.
- (29) Reference 3a, p 147. Vladimirov, A. A.; Kazakov, D. I.; Tarasov, D. V. *Sov. Phys. JETP* **1979**, *56*, 521.
- (30) Burchard, W.; Schmidt, M.; Stockmayer, W. H. *Macromolecules* **1980**, *13*, 1265.
- (31) Burchard, W. *Macromolecules* **1978**, *11*, 455.
- (32) Huber, K.; Burchard, W.; Fetters, L. J. *Macromolecules* **1984**, *17*, 541.
- (33) Flory, P. J.; Fox, T. G. *J. A. Chem. Soc.* **1951**, *73*, 1904.
- (34) Marriman, J.; Hermans, J. J. *J. Phys. Chem.* **1961**, *65*, 385.
- (35) Yamakawa, H. *Modern Theory of Polymer Solutions*; Harper & Row: New York, 1971.
- (36) Bauer, J.; Burchard, W. *Macromolecules* **1993**, *26*, 3103.
- (37) Wachenfeld-Eisele, E.; Burchard, W. *Macromolecules* **1989**, *22*, 2496.
- (38) Zimm, B. H.; Stockmayer, W. H. *J. Chem. Phys.* **1949**, *17*, 1301.
- (39) (a) Stockmayer, W. H.; Fixman, M. *Ann. N.Y. Acad. Sci.* **1953**, *57*, 334. (b) Zimm, B. H.; Kilb, R. W. *J. Polym. Sci., Polym. Phys. Ed.* **1959**, *37*, 19.
- (40) Casassa, E. F. *J. Phys. Chem.* **1962**, *37*, 2176.
- (41) Rey, A.; Freire, J. J.; Garcia de la Torre, J. *Macromolecules* **1987**, *20*, 342. Compare ref 42.
- (42) Lang, P.; Burchard, W.; Wolfe, M. S.; Spinelli, H. S.; Page, L. *Macromolecules* **1991**, *24*, 1306.
- (43) Robin, J. P.; Mercier, Ch.; Dpart, F.; Charbouniere, R.; Guilbot, A. *Starch / Staerke* **1975**, *27*, 36.
- (44) Thurn, A.; Burchard, W. *Carbohydr. Polym.* **1985**, *5*, 441.
- (45) Guilbot, A.; Mercier, Ch. In *Starch*; Aspinall, G. O., Ed.; The Polysaccharides Vol. 3; Academic Press: London, New York, 1985.

MA9450795